AIChE WILEY InterScience DISCOVER SOMETHING GREAT

MATERIALS, INTERFACES, AND ELECTROCHEMICAL PHENOMENA

Streaming Potential Characterization of LBL Membranes on Porous Ceramic Supports

Yiwei Chen, Fenjuan Xiangli, Wanqin Jin, and Nanping Xu
Membrane Science and Technology Research Center, Nanjing University of Technology, Nanjing 210009, P.R. China

DOI 10.1002/aic.11126
Published online February 20, 2007 in Wiley InterScience (www.interscience.wiley.com).

An in-situ characterization of the growth of the self-assembled polyelectrolyte membranes on the porous support was conducted by applying transmembrane streaming potential measurement via surface charge monitoring. The membranes were prepared by layer-by-layer alternative deposition of poly (allylamine hydrochloride) and poly (styrenesulfonate) on porous ceramic supports. The surface charge variations of membranes as functions of different top-assembled materials and numbers of deposited cycles were investigated. Different top-assembled materials make isoelectric points of the as-prepared membranes drift in opposite directions and also lead to symmetrical signal changes of zeta-potential in salt solutions at the isoelectric points of the supports. Ex-situ characterizations, including scanning electron microscopy, atomic force microscopy, *and energy dispersive X-ray spectroscopy, also confirm the alternative deposition of polyelectrolytes. It is demonstrated that the transmembrane streaming potential measurement is effective in studying the growth of layer-by-layer membranes on porous support.* © 2007 American Institute of Chemical Engineers *AIChE J,* 53: 969–977, 2007
Keywords: streaming potential, self-assembly, layer-by-layer, porous, composite membrane

Introduction

The layer-by-layer (LBL) alternative deposition of polyelectrolytes or other macromolecules on various supports has attracted much attention in many applications[1–3] since Decher[4,5] proposed the easy self-assembled way to build controllable thin films on charged surfaces. In the past two decades polyelectrolyte films deposited on dense substrates have been extensively studied because of its convenient characterization. Recently composite membranes prepared by LBL deposition of polyelectrolyte films on porous supports gradually become the focus of attention for prominent membrane performance[6–10] and antifouling advantage,[11] which depends to a great extent on membrane formation and surface properties. Hence, characterization of such composite membrane is of great importance.

Some of the widely employed traditional characterization techniques are scanning electron microscopy (SEM), atomic force microscopy (AFM), UV–vis, ellipsometry, X-ray reflectometry, scanning angle reflectometry, and ATR-FTIR.[6–12] These above methods provide considerable information on samples geography or special optical characters to expatiate on the fabrication of polyelectrolyte layers, but most of those are limited to certain types of depositing support material and shape, inconvenient sample preparation, and sample irreversible destruction. Specially, for composite membranes (Figure 1), the characterization methods are mostly restricted within the regions of membranes deposited on the surface of supports and do not take account into the layers adsorbed on the pore walls of supports, which also contribute a lot to performance of composite membranes.

Surface charge or electrical potential properties of a membrane have a very substantial influence on their separation performance. Experiments as well as theory have demonstrated that the rejection and antifouling behavior of a membrane depends on such properties.[7–9,13,14] Tieke and

Correspondence concerning this article should be addressed to W. Jin at wqjin@njut.edu.cn.

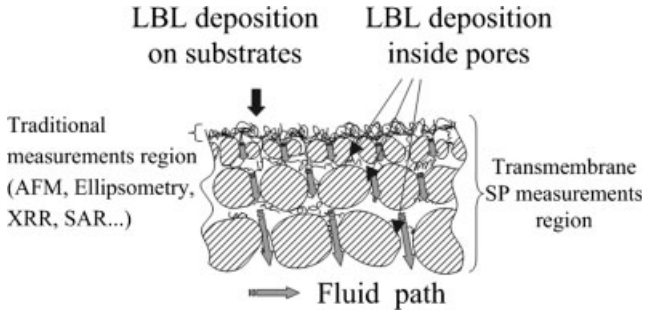

Figure 1. Comparison of the structure characteristic region of traditional methods and transmembrane SP measurement.

coworkers[8,9] observed that the charge density of polyelectrolyte is an important structural parameter controlling the membrane growth and filtration properties. Harris et al.[7] reported the LBL layers of cross-linked poly (acrylic acid)/poly (allylamine hydrochloride) (PAH) through heat-induced amidation, which provides modest corrosion protection for supports because of the special intrinsic charge compensation.

The zeta potential, which is the potential at the shearing plane between the compact layer and diffuse layer, is an important indicator of the surface charge.[15–17] The electrokinetic techniques to determine the zeta potential of charged particles or membrane surface appear as a promising method to study the charged polyelectrolyte layers. Among the electrokinetic techniques, electrophoresis measurement[18–22]was applied to determine the self-assemble deposited layers on charged particles but it was adapted to granular substrates.

Streaming potential (SP) measurement is an especially powerful electrokinetic method for the interfacial characterization on substrates of any shape.[16,17] It is a useful method to study the interactions of solid/liquid interfaces on the fluid path. It performs frequently in two ways for different objects: flowing along the top surface of membrane or flowing through the membrane pores. The first procedure, known as tangential SP measurement (on the active layer side), generally provides the unambiguous information, which only reflects the surface layer. It has been applied to study the layers on nonporous supports such as single capillary[23–25] and planar silts,[26,27] upon which the growth of layers could also be characterized by traditional methods. The second procedure, known as transmembrane SP measurement, presents the charge information on the fluid path of layer surface-layers-support pores which is identical to that during membrane processes. So, the transmembrane SP measurement can reflect the global composite membrane charge properties, which include membranes deposited on the surface of both supports and walls of support pores, and gives direct instructional knowledge on applications of the composite membranes. A schematic comparison of the characterization region of traditional methods (AFM, ellipsometry, X-ray reflectometry, scanning angle reflectometry, and so on) and transmembrane SP measurement is shown in Figure 1.

Another advantageous feature of SP measurement is that it is performed in the presence of aqueous solutions. The surfaces of polyelectrolyte membranes exhibit variable interfacial properties depending on the solution environment. With the consideration of both dissociation of functions and adsorption of salt ions as surface charge, the interface information similar to that in the self-assembly process is able to be obtained online. Moreover, SP measurement, as an in-situ method, can be carried out at any step of the LBL process without structure destruction, and membrane surface properties can be restored by a simple rinse.

As far as we know, there is no report about the characterization by applying transmembrane SP measurement on composite membrane (LBL membranes/porous support). In this work, therefore, we performed the LBL process on porous ceramic supports and then carried out transmembrane SP measurement to characterize the growth of polyelectrolyte layers. By controlling the condition of measurements, both global charge of the composite membrane and the individual influence of the self-assembled layers on the sigh of zeta potential were studied.

Theory About Transmembrane SP Measurements

Membranes acquire an electric surface charge when in contact with an aqueous solution. For the sake of electroneutrality, ions in the adjacent solution reorganize and the electrical double layer form. The potential and the ionic concentration vary progressively from the charged surface to the bulk solution. When liquid is forced through a channel (whose walls are charged) under an applied hydrostatic pressure, the charges in the mobile part of the double layer moves with the surrounding liquid, giving rise to a streaming current, I_s, and the accumulation of charge at one end sets up an electric field. The field causes a current flow in the opposite direction through the bulk of liquid and when this latter conduction current, I_c, is equal to the streaming current, a steady state is achieved ($I = I_s + I_c = 0$).[17] The resulting electrostatic potential difference between the ends of the channel is the SP.

The zeta potential, which is the potential at the shearing plane between the compact layer and diffuse layer, could be linked to the SP by the modified Helmholtz–Smoluchowski (HS) equation derived for cylindrical pores[15–17,28]:

$$\left(\frac{d\varphi_s}{dP}\right)_{I=0} = \frac{\zeta\varepsilon_0\varepsilon_r}{\eta(\lambda_0 + 2\lambda_s/r_p)} \tag{1}$$

$$\mathrm{SP} = \left(\frac{d\varphi_s}{dP}\right)_{I=0} \tag{2}$$

where ζ is the zeta potential derived from the SP, ε_0 is the electric constant (8.854×10^{-12} F m^{-1}), η is the dynamic viscosity of the solution, ε_r is the relative dielectric constant of the solution, λ_0 is the bulk salt solution conductivity, λ_s is the surface conductivity of pores, and r_p is the pore radius.

The classical HS equation (Eq. 3) is obtained when $r_p/\kappa^{-1} > 1$, where κ^{-1} is the Debye length.

$$\left(\frac{d\varphi_s}{dP}\right)_{I=0} = \frac{\zeta\varepsilon_0\varepsilon_r}{\eta\lambda_0} \tag{3}$$

Salt concentration and pore radius have been studied as predominant parameters for electrokinetic measurements.[29,30]

Table 1. Physical Property of Supports

	Top Layer/Intermediate Layer/Support	Geometry	Each Layer Thickness	Top Layer Mean Pore
Support A	ZrO_2/α-Al_2O_3/α-Al_2O_3	Tubular	20 μm/40 μm/2.5 mm	~0.2 μm
Support B	SiO_2/support A	Tubular	0.1~0.2 μm/support A	~0.1 μm
Support C	SiO_2/Si	Plane	–	–

With increasing salt concentration, a high ionic strength obtained and leads to a compression of the double layer. The double-layer length, also called as Debye length, reduced due to a screening of the surface charge at a shorter distance. More counterions can penetrate the compact layer and then fewer counterions left in the diffuse layer can be displaced under the pressure distance. As shown in HS equation, a high λ_0 leads to a small SP. Thus a lower salt concentration leads to a higher sensitivity of SP measurement but also a larger κ^{-1} (for NaCl solution, $\kappa^{-1} \approx 30.4$ nm at 10^{-4} M and $\approx$9.6 nm at 1 mM[31]). For HS equation r_p/κ^{-1} should be large enough, which means no overlap of the double layer inside the pores.

To correct a contribution of fixed part of the double layer to electrical conductivity (surface conductivity), Rice and Whitehead[28] have suggested some correction by introducing a function $F(\kappa r_p, \zeta)$. However, HS equation was commonly used by many researchers to obtain an apparent zeta potential for membrane comparison.

In this study, when applying the SP measurements we found that the flux of the composite membrane with more than 30 layers of polyelectrolytes is very low. Therefore, to avoid small r_p we restrict the number of deposition cycles in SP measurements within 15. The moderate salt concentration (1 mM) was adopted to give a small κ^{-1} and enough potential measurement sensitivity. Function F was not applied to simplify the calculation as the apparent zeta potential could clearly demonstrate the variation of surface charge.

We conducted the SP measurement at a wide pH range to study the global zeta potential of the composite membrane, which is very essential in understanding and predicting the filtration performance of a membrane. To investigate the individual influence of polyelectrolyte deposition on zeta potential, we want to relieve the effects of the supports as much as possible. Then we carried out the SP measurements at pH values of the isoelectric points (IEPs) of the supports to eliminate charge effects of the supports. One should notice that the supports still contribute to the overall signal even if they are uncharged since there is still a pressure drop through their porous structure.[32] In other words, the value of the pressure difference used in Eq. 3 is an overestimate. But we think that the contribution of the support does not affect the sign of the apparent zeta potential when measurements are carried out at the support IEPs. Consequently, the variety of the sign of the apparent zeta potential which is not further corrected in this study is able to demonstrate the growth of the polyelectrolyte multilayers.

Experimental

Materials

To study the effects of support materials on LBL process, two different porous membranes were prepared as supports in this work. Their properties are described in Table 1. Support A has a tubular geometry, made by our laboratory. Support B was prepared by a SiO_2 sol–gel modification on Support A. The top silica layer was obtained by depositing the silica sol prepared under the acid-catalyzed condition hydrolysis of tetraethyl orthosilicate (TEOS) on support A and sintered at 500°C for 2 h. A dense silicon substrate, which was chemically oxidized by a dilute Pahara solution was used as the substitutive oxide support (support C, details shown in Table 1) to meet the sample roughness requirement of AFM observation. A dilute Piranha solution (H_2SO_4:H_2O_2:H_2O, v:v:v = 1:1:3) was mixed, and the silicon wafer was ultrasonically cleaned and oxidized within this solution at ~80°C for 5~30 min. The silicon wafer was then rinsed with water and stored in water.

PAH (M_w = 70,000), poly (styrenesulfonate) (PSS) (M_w = 10,000), and polyethylenimine (PEI) (M_w = 20,000) were purchased from Aldrich. All electrolyte solutions were prepared from pure water (conductivity, <5.00 μs cm^{-1}), and the other reagents were of analytical grade and were used without further purification.

Self-assembly of polyelectrolyte on porous supports

Polyelectrolytes were dissolved in water at a concentration of 2×10^{-2} monomoles/l (monomole = mole of monomer unit) and acidified to a certain pH (pH = 2 for this study) for each pairs of electrolytes using aqueous HCl.

Surface pretreatments of supports were of great necessary as to get uniform and enough charged sites. Supports were first treated in boiled pure water for 15 min and rinsed to get rid of any adhesive impurity. After soaked in acetone, the supports were transferred to the dilute Piranha solution at ~60°C for 5~30 min. Then the supports were thoroughly rinsed with water and stored in water.

To enhance the adsorption of the individual layers, the pretreated supports were first immersed in PEI solution for 30 min and then rinsed in water. Afterward the supports were immersed in sequence (a) in the solution of the PSS, (b) in water (pH = 2), (c) in the solution of the PAH, and (d) in water (pH = 2) again. Steps (a) to (d) were repeated until a concern numbers of deposition cycles of PAH/PSS were absorbed and ultimately rinsed in water and dried by N_2. The dipping time for every polyelectrolyte solution was 30 min and the rest time in water was 5 min.

Transmembrane SP measurements

Transmembrane SP measurements were used to determine the surface potential of the composite membrane. The apparatus presented schematically in Figure 2 consisted of two reversible Ag/AgCl electrode compartments installed at both sides of the membrane. A precise pressure sensor is also used at the feed side. The pH of NaCl solution was regulated

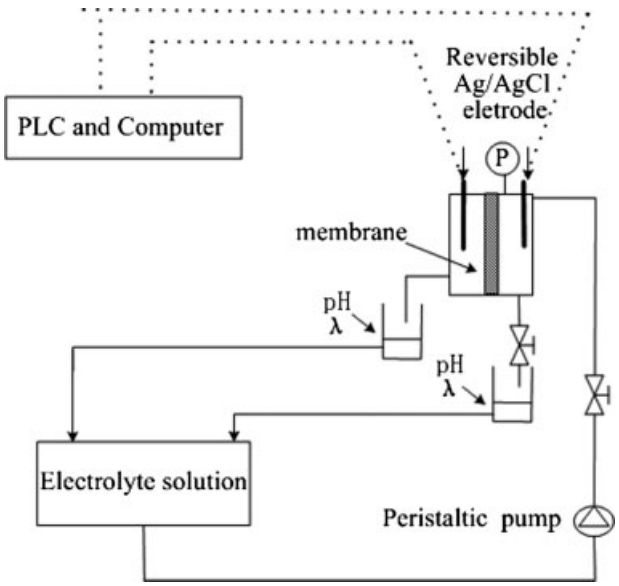

Figure 2. Experimental unit for transmembrane streaming potential measurements.

by addition of hydrochloric acid or sodium hydroxide. Composite membranes were soaked overnight in electrolyte solution under the consideration to equilibrate it with measuring solution.

The SP measurements were carried out by increasing transmembrane pressure pulses ranging from 0.005 to 0.025 MPa and measuring the variation of resulting electrical potential difference on both sides on the composite membrane. Online data collection of electrical potential was obtained with a software package of Step 7-Micro/win32 (Siemens Energy&Automation, Inc.) via a Simatic S7-200 PLC connected to the Ag/AgCl electrodes. All measurements were performed at ambient temperature with the help of circular water.

Ex-situ characterizations

To obtain the morphologies of the LBL membranes and confirm the deposition process, ex-situ characterizations were performed by SEM and energy dispersive X-ray spectroscopy (EDXS). AFM was also carried out to obtain complementary information on the growth of polyelectrolyte multilayers on oxide surface. For AFM observation a dense silicon substrate covered by a thin layer of SiO_2 (support C), which had been chemically oxidized by a dilute Piranha solution, was used as a substitutive support to meet the sample roughness requirement. Though the structural differences between the porous and dense supports affect the morphology of the polyelectrolyte layers, we could also obtain important information on the growth of polyelectrolyte layers since all the support we used have similar oxide composition of surfaces.

Both surface morphologies of the supports and the self-assemble layers were characterized using a SEM (QUANTA-2000). An EDXS was used for chemical analysis of the deposited layers. The growth of the self-assemble layers on the substitutive oxide support was characterized using a multimode AFM (Autoprobe CP-Research system, Veeco Instruments).

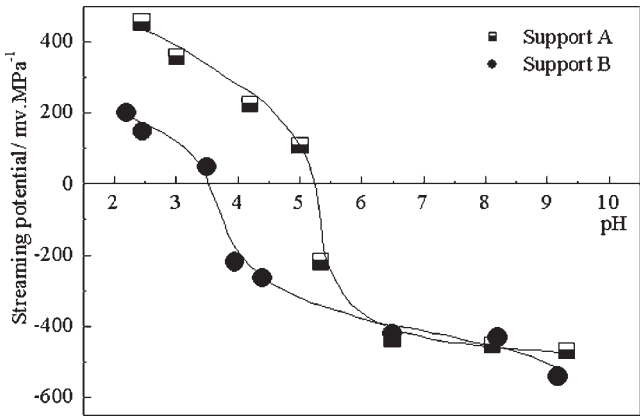

Figure 3. Variation of pH dependence of streaming potential for support A and support B.

Salt solution: 1 mM NaCl.

Results and Discussion

Transmembrane SP measurements

Porous Supports. The original charge properties of supports A and B were first studied. The SP variations for supports A and B versus pH in a NaCl solution of 1 mM is shown in Figure 3. The pH dependence of the SP can be explained by the shifting of the proton equilibrium that occurs at the surface of membrane when pH moves. This modifies the net charge of the surface as well as the number of the counterions in the diffuse layer and then SP variation accompanies.

As shown in Figure 3, without polyelectrolyte deposition, IEP values of the supports A and B are close to 5.2 and 3.5, respectively. Table 2 lists the pH (IEP) values reported in the literatures for the three oxides used for our supports. The IEPs of the supports are close to those of the top layer oxides and there seems little influence of the support and intermediate layer. It may be due to the large difference of pore radii and transport properties between the various layers. It is normally assumed that the thin top layer controls the water and salt flux, and that the higher of the pore radius ratio ($r_{support}/r_{top}$), the larger pressure drop across the top layer. The pressure-induced SP is thus greatly dependent on the potential of the top layer.

The global potential is determined by the competition of the effects of the support and the top layer. The contribution of the support layer could not be neglected since the ratio of the hydraulic permeabilities of the support and the top layer is not high enough (in the case of Support A, is 1.8). Therefore, each IEP of the two supports is intermediate between the individual IEP of the top layer and the support layer, and is observed more close to that of the top layer in this study.

Self-Assembled Layers on Porous Supports. We carried out the measurement at a wide pH range to study the variations of global charge information of the composite mem-

Table 2. pH (IEP) of the Used Oxides

Oxide	pH (IEP)	Reference
Al_2O_3	8.75–9.4	33
SiO_2	2–4	33
ZrO_2	4–5.1	34

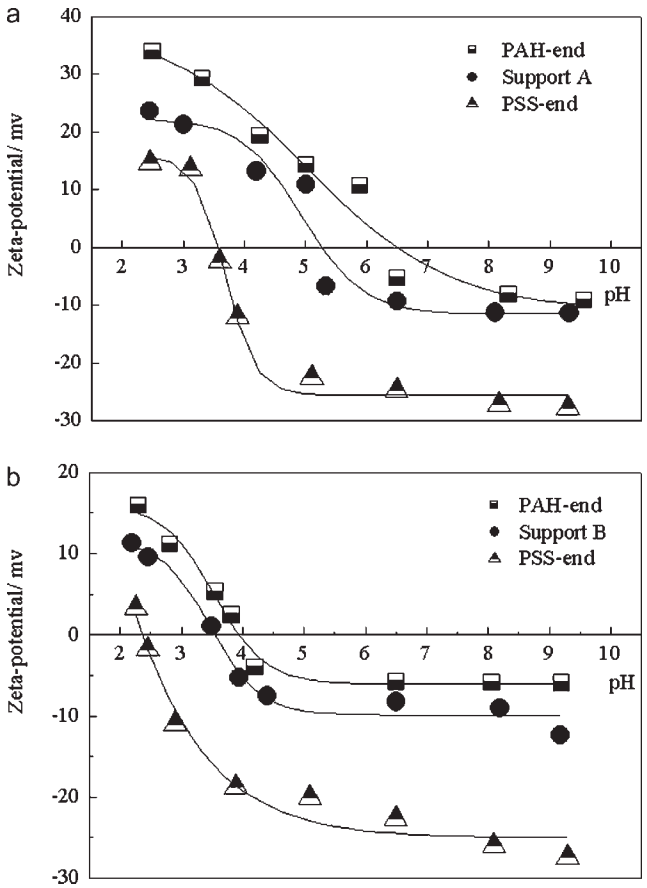

Figure 4. Effect of top-materials on the pH dependence of zeta potential for (a) support A and (b) support B after 10 deposition cycles of PAH/PSS.

Salt solution: 1 mM NaCl.

branes after LBL process. Figure 4 shows the IEP drifts after deposition of 10 cycles of PAH/PSS multilayers on the supports A and B. For the support A, when the positive-charged PAH was deposited as the top-material, the IEP drifts from 5.2 to 6.3 while the negative-charged PSS makes the IEP drift obviously to 3.6. The similar results could be viewed in Figure 4b for the support B. IEP drifts of support B are from 3.5 to 4 and to 2.4 for PAH and PSS respectively.

Symmetrical potential changes were observed in dilute salt concentrations at a fixed pH when opposite-charged polyelectrolytes were deposited on a dense silica capillary surface.[23–25] However, the variation of zeta potential in this study seemed not as sharp as that reported in literature.[23–25] It is due to the noticeable difference of deposition condition. First, the used ceramic supports are different from dense substrates since they are porous medium with a large specific area and a rough membrane surface. The deposition of polyelectrolytes on this substrate should take place both upon the porous surface and inside the pores (Figure 1). Consequently, considerable amounts of charged sites on the support still remained, which were not covered by the polyelectrolytes, while the amounts of remaining charged sites were much less in a capillary with a dense surface. Second, the measurements reported in the literature[23–25] were restrict at a fixed pH, upon which data analysis could only give incomplete information of membrane surface, while the measurements here were conducted in a wide pH range and global charge information were obtained.

As is also shown in Figure 4, the zeta potentials decrease with raising pH and the decreasing rates become smaller at pH higher than the IEPs of supports. Furthermore, greater IEP drifts are caused by PSS than by PAH. This is attributed to the difference of pKa values between the two polyelectrolytes. As a weak polybase and only 50% of the polar groups ionized at a narrow pH range under pH $\approx$ 3.3,[35] PAH segments deposited on the surfaces was partly charged within pH range of IEP measurement while PSS was fully ionized in this case. Thus PAH affects less than PSS on counter-ions transfer at measurement condition. As the PSS is fully ionized in a wide pH region, the zeta potential would be hardly affected by pH when PSS is the top material of the membrane. In other words, we would expect ζ = constant (<0) in a wide pH region. But we only observed the slow decrease at high pH because of the important contribution of remaining sites on the supports.

At IEPs of Supports. As discussed above, the global charge information on the composite membrane includes

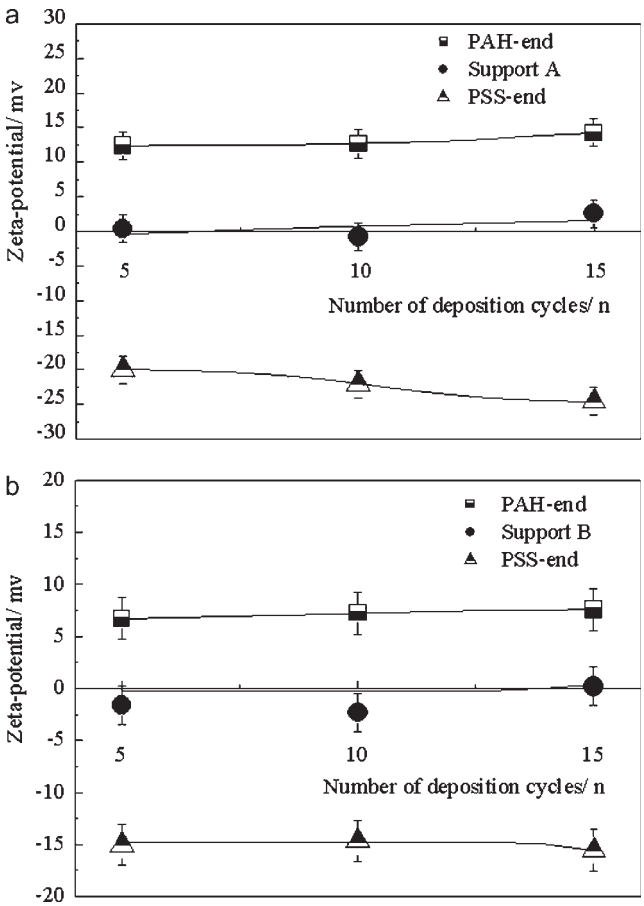

Figure 5. Effect of top-materials on the deposition cycle number dependence of zeta potential at IEP of (a) support A and (b) support B for PAH/PSS layers.

Salt solution: 1 mM NaCl.

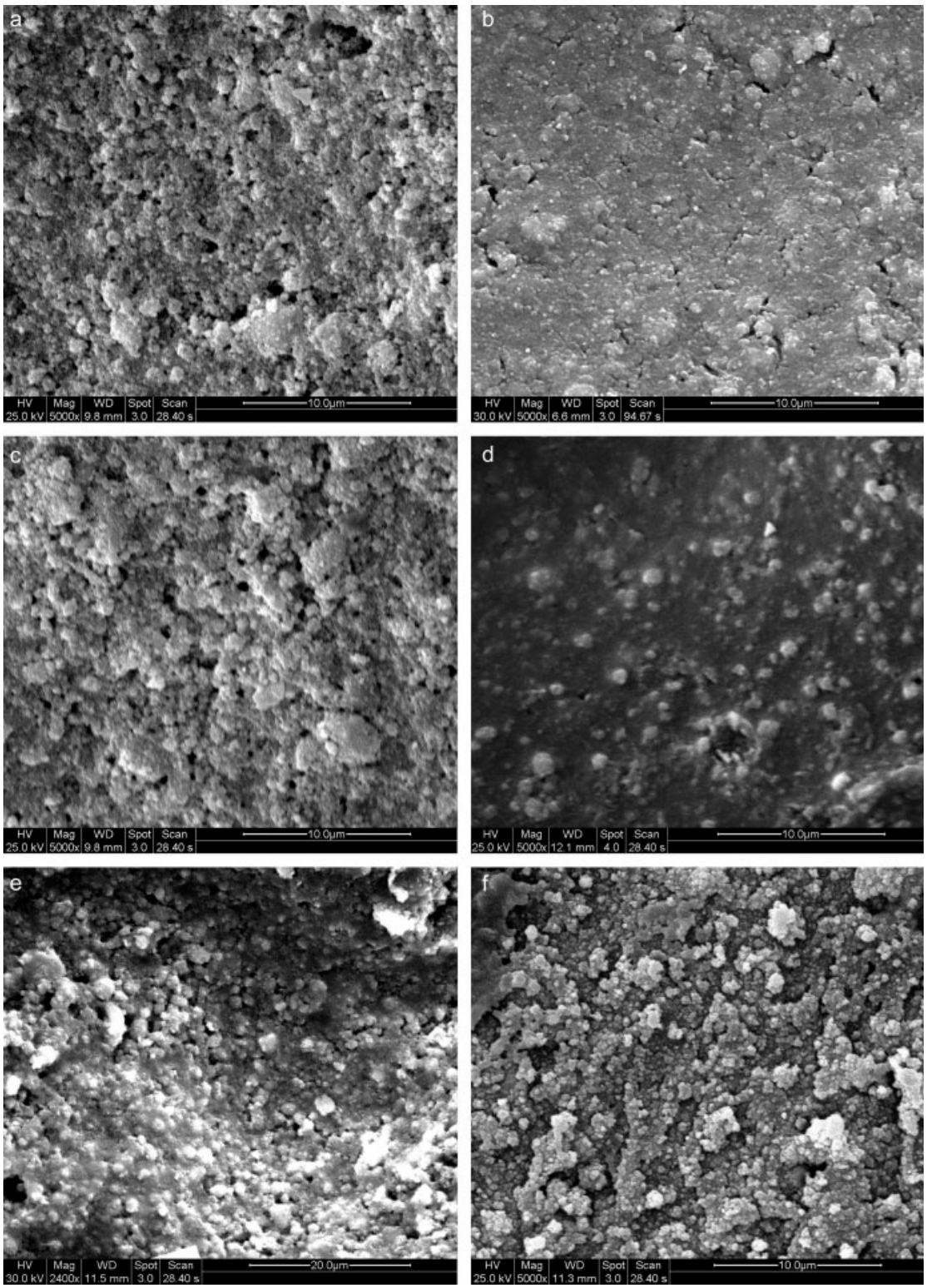

Figure 6. SEM images of the membranes.

(a) Surface of support A; (b) surface of support B; (c) surface of 10 deposition cycles of PAH/PSS on A; (d) surface of 10 deposition cycles of PAH/PSS on B; (e) surface of 40 deposition cycles of PAH/PSS on A; and (f) surface of 40 deposition cycles of PAH/PSS on B.

effects of the supports, which helps us to study the actual properties of the membranes during separation applications, but interferes with the individual study on the growth of self-assembled membranes. Then we attempt to quantitate the effects of polyelectrolytes on zeta potential by mathematical calculation.

A surface chemical composition accounts for the global charge property of composite membrane. An equation

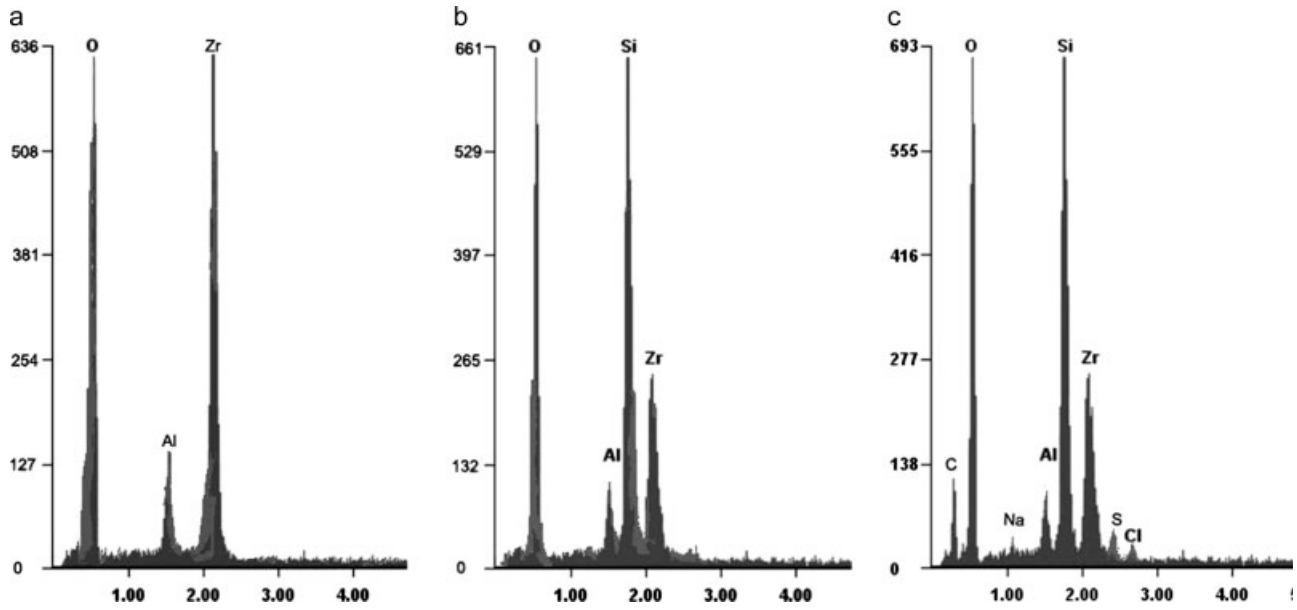

Figure 7. EDXS analysis of membrane surfaces.

(a) Support A (b), support B, and (c) 40 deposition cycles of PAH/PSS on support B.

derived by Furlong et al. was widely used to correlate the IEP of membrane[33]:

$$\mathrm{pH}(\mathrm{IEP}_{\mathrm{membrane}}) = \sum_i x_i \mathrm{IEP}(i) \tag{4}$$

where x_i is the molar ratio of the surface sites of membrane material i and it assumes a linear relationship between the pH(IEP) and surface concentration of sites.

For the composite membrane here, the porous supports present multilayer structure of several types of oxide. Mixed surface charged sites have formed after polyelectrolyte deposition on the support surface and on the pore walls. Thus, both oxides and polyelectrolytes will contribute to the global SP, which depends on competition for aspects motioned above, including charged degrees at various pH values, oxide natures, and charged sites distribution in various layers with different pore radii and thickness fraction. Hence, it is difficult to quantitate the polyelectrolyte part of the global zeta potential by simple mathematical means. Therefore, it is necessary to screen the influence of supports for the sake of eliminating aspects motioned above which concern supports.

To relieve the effects of the supports as much as possible, we applied SP measurements using a salt solution at pH values of the IEPs of the supports. At this pH value, the net charge of support oxide is equal to zero and the charge effects of support sites could be neglected, though there is still some pressure effects of the supports left which would not affect the sigh of the apparent zeta potential. Therefore, the influence of polyelectrolyte layers on the sigh of zeta potential of the composite membrane could be studied.

We studied the zeta potential variation of the composite membrane with different top-materials and various numbers of deposition cycles. Figure 5 shows the effects of top-material and the number of deposition cycles of polyelectrolytes on the zeta potential variation at the IEPs of the two supports. From Figure 5, the symmetrical opposite potential signal changes present clearly with different top-materials as expected, which is consistent with literature.[22–25] A moderate salt solution (1 mM) was used here and the magnitude of zeta potential was in agreement with values reported by others.[22–25] The zeta potential represents the net charge density of the membrane surface, which determines the subsequent deposition of opposite charged polyelectrolyte. For successive alternative deposition, the absolute net charge each polyelectrolyte brings to the surface should be same for the polyanion and polycation so that charge overcompensation could happen circularly. One could observe that the zeta potential absolute values of PAH are always lower than that of PSS for the supports A and B. This is attributed to the fact that the pH values at which PAH is partially ionized while PSS is fully ionized are far away from the pH values during deposition process.

As shown in Figure 5, the absolute value of zeta potential increased slightly with increasing the numbers of polyelectrolyte deposited cycles. There seems to be a trend of zeta potential to approach a stable value. It implies that the defect of polyelectrolyte layers is mending during the process of deposition because of more extent of the polyelectrolytes covered on the fluid path. As a consequence, more active sites of polyelectrolytes contribute to the zeta potential at this pH value and make the absolute value of zeta potential increase.

Ex-situ characterization for comparison

From surface charge information obtained by SP measurement, we can expatiate on the self-assembly of polyelectrolyte layers on porous supports via electrochemical analysis. To confirm the layers deposition through intuitionistic morphology observation, SEM and AFM were carried out as complementary methods. EDXS analysis was also performed to analyze the components of the composite membrane surface.

The images of the fresh supports obtained by SEM are shown in Figures 6a, b. The surface of support A (Figure 6a) shows a somewhat rough and uneven surface with big par-

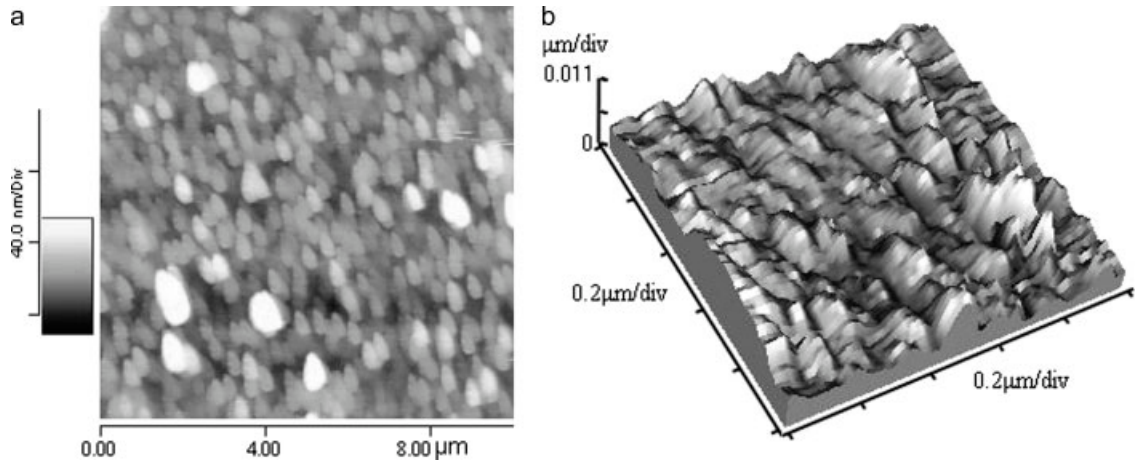

Figure 8. AFM images of the membrane surfaces.

(a) Phase image of 40 deposition cycles of PAH/PSS on support C; (b) height image of (a).

ticles of ZrO_2. The surface of support B (Figure 6b) shows a more even. Figures 6c–f show the surface image of PAH/PSS layers on supports. Figures 6c, d show the images of the support A and B after deposition of 10 cycles of PAH/PSS, respectively. Difference between the surface images of the fresh supports and the deposited polyelectrolytes could be observed. Especially, some sparse islands of polyelectrolytes appear at the surface of support B (Figure 6d) with discrete distribution. It indicates that the defect-free layers have not formed by such scale of deposition, which is consistent with what was discussed above. The surface of the deposition of 40 cycles of PAH/PSS on the supports A and B (Figures 6e, f, respectively) show that clusters have encountered each other to form and arrange clumpy layers.

Figures 7a and b show element analysis of the chemical species on the porous supports. A fresh surface of support A shows a great Zr region and some content of Al. After the modification of the silica layer, the Si region becomes absolutely dominant accompanied with Zr region decrease and still some Al, which to some extent affects the zeta potential of the composite membrane as discussed above. The deposition of polyelectrolytes is confirmed from Figure 7c, from which we could observe that some regions of C, Na, S, and Cl emerge. As the membranes have been thoroughly rinsed with water after deposition, there are no excess ionized PAH or PSS molecules left on the supports. The appearance of S region is due to the self-assembled PSS, and the moderate C region declares polyelectrolyes deposition. Under the condition of general ionization of PAH and PSS, Na and Cl mostly remain ionic states as Na^+ and Cl^- respectively during the self-assembly process. Their emergences here can be explained by some degree of the extrinsic charge compensation[36] in the deposited polyelectrolyte multilayers and some unionized parts of the multilayers.

Figure 8 shows the surface structure of the self-assemble polyelectrolyte layers on support C from AFM measurements. Figure 8a is phase image of the 40 deposition cycles of PAH/PSS on the support C and Figure 8b is the topography image for Figure 8a. As shown in Figures 8a, b, the geology presents rough and jagged with randomly distributed small particles and isolated peaks. Since the pretreated substrate has a smooth and even topography in the scale of several nanometers, the formation of the peaks must be a consequence of the subsequent polyelectrolyte deposition. There seem to be two mechanisms during the deposition. On one hand, when the series of opposite charged polyelectrolytes are approaching the charged surface, the tendency for reducing surface energy and the steric hindrance caused by the branched structure of charged polyelectrolytes leads the deposition to take place in a homogenous manner. On the other hand, the possible inhomogeneous charge distribution of substrates surface causes isolated deposition which will limit the growth rates of sequent deposition and lead to clusters and large 3D aggregation in these isolated areas.

Conclusion

Our studies indicate that the transmembrane SP measurement is an effective method to investigate the LBL growth of polyelectrolytes deposited on porous ceramic supports. The global IEP drifts were found after LBL deposition of PAH/PSS on supports. When the positive charged material (PAH) deposited as the top-material, the IEP drifts to a high pH value while the negative charged material PSS does the reverse. After eliminating the charge effects, the symmetrical potential signal change was observed for opposite charged top-material which indicates the growth of polyelectrolyte layers. The amplitude of zeta potential shows a slight increase with increasing number of deposition cycles of polyelectrolytes.

SEM and AFM observations demonstrate the surface modifications by LBL deposition on porous and dense supports respectively. EDXS analysis indicates polyelectrolyte segments have successfully deposited on the porous supports.

A further work for detailed effects of supports and polyelectrolytes on charge property of composite membrane surface will be investigated.

Acknowledgments

This work is sponsored by the National Basic Research Program of China (No. 2003CB615702), National Natural Science Foundation of China (NNSFC, No. 20446002, 20436030), Natural Science Foundation of Jiangsu (BK2006722), and the Key Laboratory of Material-Oriented Chemical Engineering of Jiangsu Province and Ministry of Education.

Notation

I = electric current, A
I_c = conduction current, A
I_s = streaming current, A
P = hydrostatic pressure, N m^{-2}
pKa = negative log of acid dissociation constant
r_p = pore radius, m
r_{top} = pore radius of top layer, m
$r_{support}$ = pore radius of support layer, m
SP = streaming potential, V N^{-1} m^{-2}
x_i = molar ratio of the surface sites of membrane material i

Greek letters

ε_0 = electric constant, F m^{-1}
ε_r = relative dielectric constant of the solution
κ = Debye parameter, m^{-1}
κ^{-1} = Debye length, m
λ_0 = bulk salt solution conductivity, Ω^{-1} m^{-1}
λ_s = the surface conductivity of pores, Ω^{-1}
η = dynamic viscosity of the solution, kg m^{-1} s^{-1}
φ_s = electrical potential, V
ζ = zeta potential, V

Literature Cited

1. Hammond PT. Recent explorations in electrostatic multilayer thin film assembly. *Curr Opin Coll Interface Sci*. 2000;4:430–442.
2. Decher G, Schlenoff JB. Multilayer thin films. In: Decher G, editor. *Polyelectrolyte Multilayers, An Overview*. Weinheim: Wiley-VCH, 2003:1–46.
3. Schönhoff M. Self-assembled polyelectrolyte multilayers. *Curr Opin Coll Interface Sci*. 2003;8:86–95.
4. Decher G, Hong JD. Buildup of ultrathin multilayer films by a self-assembly process. I. Consecutive adsorption of anionic and cationic bipolar amphiphiles. *Macromol Chem Macromol Symp*. 1991;46: 321–327.
5. Decher G. Fuzzy nanoassemblies: toward layered polymeric multicomposites. *Science*. 1997;277:1232–1237.
6. Sullivan DM, Bruening ML. Ultrathin, cross-linked polyimide pervaporation membranes prepared from polyelectrolyte multilayers. *J Membr Sci*. 2005;248:161–170.
7. Harris JJ, Stair JL, Bruening ML. Layered polyelectrolyte films as selective, ultrathin barriers for anion transport. *Chem Mater*. 2000; 12:1941–1946.
8. Toutianoush A, Krasemann L, Tieke B. Polyelectrolyte multilayer membranes for pervaporation separation of alcohol/water mixtures. *Colloids Surf A: Physicochem Eng Asp*. 2002;198–200:881–889.
9. Jin WQ, Toutianoush A, Tieke B. Use of polyelectrolyte layer-by-layer assemblies as nanofiltration and reverse osmosis membranes. *Langmuir*. 2003;19:2550–2553.
10. Nagale M, Kim BY, Bruening ML. Ultrathin, hyperbranched poly (acrylic acid) membranes on porous alumina supports. *J Am Chem Soc*. 2000;122:11670–11678.
11. Müller M, Rieser T, Lunkwitz K, Berwald S, Haack JM, Jehnichen D. An in-situ ATR-FTIR study on polyelectrolyte multilayer assemblies on solid surfaces and their susceptibility to fouling. *Macromol Rapid Commun*. 1998;19:333–336.
12. Caruso F, Furlong DN, Ariga K, Ichinose I, Kunitake T. Characterization of polyelectrolyte-protein multilayer films by atomic force microscopy, scanning electron microscopy, and Fourier transform infrared reflection-absorption spectroscopy. *Langmuir*. 1998;14:4559–4565.
13. Moritz T, Benfer S, Arki P, Tomandl G. Influence of the surface charge on the permeate flux in the dead-end filtration with ceramic membranes. *Sep Purif Technol*. 2001;25:501–508.
14. Wang M, Wu LG, Zheng XC, Mo JX, Gao CJ. Surface modification of phenolphthalein poly(ether sulfone) ultrafiltration membranes by blending with acrylonitrile-based copolymer containing ionic groups for imparting surface electrical properties. *J Colloid Interface Sci*. 2006;300:286–292.
15. Hunter RJ. *Zeta Potential In Colloid Science: Principles And Applications*. London: Academic Press, 1981.
16. Fievet P, Szymczyk A, Labbez C, Aoubiza B, Simon C, Foissy A, Pagetti J. Determining the zeta potential of porous membranes using electrolyte conductivity inside pores. *J Colloid Interface Sci*. 2001; 235:383–390.
17. Szymczyk A, Fievet P, Aoubiza B. Electrolyte conductivity in charged capillaries. *Desalination*. 2002;151:177–l84.
18. Graul TW, Schlenoff JB. Capillaries modified by polyelectrolyte multilayers for electrophoretic separations. *Anal Chem*. 1999;71: 4007–4013.
19. Voigt A, Lichtenfeld H, Sukhorukov GB, Zastrow H, Donath E, Bäumler H, Möhwald H. Membrane filtration for microencapsulation and microcapsules fabrication by layer-by-layer polyelectrolyte adsorption. *Ind Eng Chem Res*. 1999;38:4037–4043.
20. Schwarz B, Schönhoff M. Surface potential driven swelling of polyelectrolyte multilayers. *Langmuir*. 2002;18:2964–2966.
21. Caruso F, Donath E, Möhwald H. Influence of polyelectrolyte multilayer coatings on förster resonance energy transfer between 6-carboxyfluorescein and rhodamine B-Labeled particles in aqueous solution. *J Chem Phys B*. 1998;102:2011–2016.
22. Burke SE, Barrett CJ. Acid-base equilibria of weak polyelectrolytes in multilayer thin films. *Langmuir*. 2003;19:3297–3303.
23. Ladam G, Schaad P, Voegel JC, Schaaf P, Decher G, Cuisinier F. In situ determination of the structural properties of initially deposited polyelectrolyte multilayers. *Langmuir*. 2000;16:1249–1255.
24. Picart C, Lavalle P, Hubert P, Cuisinier FJG, Decher G, Schaaf P, Voegel JC. Buildup mechanism for poly(L-lysine)/hyaluronic acid films onto a solid surface. *Langmuir*. 2001;17:7414–7424.
25. Zhang J, Senger B, Vautier D, Picart C, Schaaf P, Voege JC, Lavalle P. Natural polyelectrolyte films based on layer-by layer deposition of collagen and hyaluronic acid. *Biomaterials*. 2005;26:3353–3361.
26. Chan YHM, Schweiss R, Werner C, Grunze M. Electrokinetic characterization of oligo- and poly(ethylene glycol)-terminated self-assembled monolayers on gold and glass surfaces. *Langmuir*. 2003; 19:7380–7385.
27. Schwarz HH, Lukas J, Richau K. Surface and permeability properties of membranes from polyelectrolyte complexes and polyelectrolyte. *J Membr Sci*. 2003;218:1–9.
28. Rice CL, Whitehead R. Electrokinetic flow in a narrow cylindrical capillary. *J Phys Chem*. 1965;69:4017–4024.
29. Szymczyk A, Fievet P, Reggiani JC, Pagetti J. Characterisation of surface properties of ceramic membranes by streaming and membrane potentials. *J Membr Sci*. 1998;146:277–284.
30. Zhang YP, Xu TW. An experimental investigation of streaming potentials through homogeneous ion-exchange membranes. *Desalination*. 2006;190:256–266.
31. Lyklema J. *Fundamentals of Interface and Colloid Science*, *Vol*. I: *Fundamentals*. London: Academic Press, 1991.
32. Szymczyk A, Labbez C, Fievet P, Aoubiza B, Simon C. Streaming potential through multilayer membranes. *AIChE J*. 2001;47:2349–2358.
33. Furlong DN, Freeman PA, Lou ACM. The adsorption of soluble silica at solid-aqueous solution interfaces: I. Leaching from glass—an electrokinetic study. *J Colloid Interface Sci*. 1981;80:20–31.
34. Vallar S, Houivet D, Fallah JE, Kervadec D, Haussonne JM. Oxide slurries stability and powders dispersion: optimization with zeta potential and rheological measurements. *J Eur Ceram Soc*. 1999;19: 1017–1021.
35. Krasemann L, Toutianoush A, Tieke B. Self-assembled polyelectrolyte multilayer membranes with highly improved pervaporation separation of ethanol/water mixtures. *J Membr Sci*. 2001;181:221–228.
36. Schlenoff JB, Dubas ST. Mechanism of polyelectrolyte multilayer growth: charge overcompensation and distribution. *Macromolecules*. 2001;34:592–598.

Manuscript received Oct. 9, 2006, and revision received Dec. 14, 2006.